Available online at www.sciencedirect.com
SCIENCE DIRECT®
Polymer 45 (2004) 217–229
polymer
www.elsevier.com/locate/polymer

Oriented structure and anisotropy properties of polymer blown films: HDPE, LLDPE and LDPE

X.M. Zhang*, S. Elkoun, A. Ajji, M.A. Huneault

National Research Council Canada-IMI, 75 boul. de Mortagne, Boucherville, Québec J4B 6Y4, Canada

Received 17 June 2003; received in revised form 29 September 2003; accepted 6 October 2003

Abstract

Different types of polyethylene blown films (HDPE, LDPE, LLDPE) differ significantly in the ratio between machine and transverse direction tear resistance. In this paper, low density polyethylene (LDPE), linear low density polyethylene (LLDPE) and high density polyethylene (HDPE) blown films at different draw-down ratios are studied, and the relation between crystalline structure and anisotropy of blown film properties is investigated. The crystalline morphology and orientation of HDPE, LDPE, LLDPE blown films were probed using microscopy and infrared trichroism. Significant differences in crystalline morphology were found: at medium DDR HDPE developed a row-nucleated type morphology without lamellar twisting, LDPE showed rod-like crystalline morphology and turned out to the row-nucleated structure with twisted lamellae at high draw-down ratio (DDR), while a spherulite-like superstructure was observed for LLDPEs at all processing conditions. They also showed quite different orientation characteristics corresponding to different morphologies. The morphologies and orientation structure for LDPE, LLDPE and HDPE are related to the stress applied (DDR) and their relaxations in the flow-induced crystallization process, which determine the amount of fibrillar nuclei available at the time of crystallization and therefore, the final crystalline morphology. These structure differences are shown to translate into different ratios of machine and transverse direction tear and tensile strengths.

Keywords: Polyethylene blown films; Crystalline morphology; Tear strength

1. Introduction

Polyethylene is used in a number of applications including flexible film packaging produced by the blown film process. Significant differences in physical properties have been observed in low density polyethylene (LDPE), linear low density polyethylene (LLDPE) and high density polyethylene (HDPE) blown films. Structural parameters, such as density/crystallinity, molecular weight and its distribution, short chain branching (SCB)/ long chain branching (LCB) length and amount and crystalline morphology are the key factors that control the properties. HDPE is the most crystalline PE, since its chains are linear and contain very little branching. It shows high modulus, medium tensile properties, poor impact and tear resistance. LDPE containing LCB in the order of 1–3 per 1000 carbon atoms as well as 10–30 SCB per 1000 C shows low tensile strength and modulus, medium impact and tear resistance. LLDPE have a wide range of SCB, depending on the type of catalyst and comonomers (butene, hexene or octene), it generally has good tensile, impact and tear resistance, the type and amounts of SCB have a significant effect on the physical properties.

Structure of polyethylene blown films has been studied for nearly 4 decades, but concerns and controversy still exist, and some structural features and physical behaviours are not completely understood. Two different structure models were proposed for PE blown film: row-nucleated structure [1] and *a*-axis structure [2]. The row-nucleated structure model of Keller and Machin [1] has been widely adopted to understand the orientation of PE blown films [3], some studies, however, favoured the *a*-axis structure model [4,5] or a modified row-nucleated structure model [6,7].

Based on row-nucleated structure model, two major crystallizations can happen upon the magnitude of the stress in the blowing process [1–10]. Low stress often results in

* Corresponding author.

0032-3861/$ - see front matter
doi:10.1016/j.polymer.2003.10.057

lamellae growing laterally outward in the form of twisted ribbons with the growth direction parallel to *b*-axis and a preferential orientation of the *a*-axis toward MD, named Keller/Machin 1 morphology (a-texture) [1]. High stress produces, so called Keller/Machin 2 morphology (c-texture) [1] in which the radially grown lamellae extend directly outward without twisting, and the regularly folded chains within lamellae remain toward machine direction. The Keller/Machin 1 morphology is the most commonly observed in PE blown films, the X-ray studies have shown this type of morphology for LDPE [6,9], HDPE [10] and LLDPE [7,8]. There is a general agreement in literature that LLDPE [7,8] and LDPE [6,9] blown films have a preferential orientation of crystalline *a*-axis to the machine direction. No studies were directed to demonstrate the difference in LDPE vs. LLDPE orientation structure, especially on the *c*-axis orientation and lamellar arrangement. Kwack et al. [12], on the other hand, reported that neither LDPE nor LLDPE showed row nucleated structure, even though both of them demonstrated *a*-axis orientation parallel to MD and *b*-axis orientation perpendicular to MD. The Keller/Machin 2 morphology has been only observed in some HDPE blown films [10,11], where *c*-axis is oriented preferentially to MD with the folded chains in the lamellae parallel to the extended microfiber and the radially grown lamellae are non-twisted. The HDPE row-nucleated morphology and *c*-axis structure has been observed [11]. Lindenmeyer [3] showed, however, both the orientation for LDPE and HDPE are essentially the same at low BUR, with both *a*- and *c*-axes being in the machine direction but inclined an angle out of the plane of the film. To get a better understanding of microstructure and properties, further studies on LDPE, LLDPE and HDPE blown films are very necessary.

Tear resistance is one of important properties for the package application films. LDPE, HDPE and LLDPE show different trends in tear resistance behaviour: LDPE blown film generally shows medium tear resistance with MD tear strength > TD tear strength, LLDPE have superior tear resistance with TD tear > MD tear resistance, finally, HDPE shows high TD tear and extremely low MD tear. No reports can be found to explain these differences. To the best of our knowledge, this is the first effort to address it from the structural point of view. In order to better clarify the morphological features developed in PE blown films and their incidence on properties, this work is directed toward the elucidation of the different behaviour in tear resistance of PE blown films. One LDPE, 3 LLDPEs were used and processed at different draw-down ratios, and one HDPE was also studied for comparison. An additional objective of this work is to study the flow-induced crystallization and orientation behaviour for the different polyethylenes (LDPE, HDPE and LLDPE), and to examine the effect of stress in machine direction and relaxation times on the fibrillar nucleated structure and on the final morphology.

2. Experimental section

2.1. Materials and blown film preparation

In this study, one LDPE, and three LLDPEs with similar melt index and density were used. The materials were provided by Nova Chemicals Corporation. The LDPE is Novapol LF-Y819. The three LLDPEs differ in terms of comonomer or catalyst. The first one is a butene based Ziegler–Natta (Z/N) catalyzed copolymer traded under the name PF-0018-F. The second one is an octene based Z/N catalyzed copolymer EX-FG120-A05. The third one is a pilot-plant 'single site' catalyzed material also produced with an octene comonomer. The three LLDPEs will be referred to as LLDPE-B, -O and -M in the following sections. One HDPE (DMDF6200) from Petromont with melting index of 3.4 g/10 min was also studied. Most studies on HDPE blown films in literature used relatively higher molecular weight HDPE, which generally shows *c*-axis structure. The HDPE used in this work has relatively lower melt index. Some characteristics of materials were listed in Table 1.

The films were produced using a Brampton Engineering extrusion blowing line. The output, blow-up ratio, die gap are fixed for all the films, draw-down ratios, however, change from low, medium to the highest possible. The processing conditions for the films are given in Table 2. The frost-line height defines the height from die to the point where crystallization starts. For all the films, the lowest frost-line height possible is used to minimize the relaxation of the orientation.

2.2. Rheological characterization

Dynamic shear rheology experiments were performed using a Rheometric Scientific ARES plate–plate rheometer. The complex viscosity vs. frequency were measured in the $0.1-100\ s^{-1}$ frequency range. Prior to performing frequency sweeps, strain sweeps were performed to establish the linear viscoelastic region.

2.3. FTIR trichroism

To understand the orientation of the blown films, it is necessary to determine their FTIR spectra corresponding to the machine (M), transverse (T) and normal (N) directions. M and T spectrum (S_M and S_T) can be easily obtained by using a planarly polarized beam with the electric vector in the desired direction. For example, specimens were put perpendicular to the FTIR beam with a vertical machine direction and horizontal transverse direction, and the measurements were performed with radiation polarized in the M and T direction, respectively. This allows the determination of S_M and S_T. The normal spectrum was obtained using the tilted method [13,14], i.e. the films were tilted by 45°, and S_N was calculated by the following

Table 1
Some characteristics of polyethylenes used in this work

Resins	M_n (kg/mol)	M_w (kg/mol)	M_w/M_n	Comonmer content (mol%)	Melt index (g/10 min)	Densty (g/cc)	T_m (°C)	T_c (°C)
LLDPE-O	30,500	10,3200	3.38	5.4	1.0	0.920	121.9	104.1
LLDPE-B	35,800	10,1600	2.84	3.5	1.0	0.918	122.3	104.5
LLDPE-M	41,000	89,700	2.19	2.8	1.0	0.917	110.6	95.2
LDPE	20,800	18,9200	9.10	–	0.75	0.920	107.6	94.8
HDPE		–	–	–	3.40	0.955	130.0	119.0

expression [14]:

$$S_N = \frac{\cos\beta}{\sin^2\beta}(S_{TN} - S_T\cos\beta) \quad (1)$$

where

$$\sin\beta = \frac{\sin 45^\circ}{n} \quad (1a)$$

and

$$S_{TN} = \frac{(S_T\cos^2\beta + S_N\sin^2\beta)}{\cos\beta} \quad (1b)$$

and n is refractive index of the polymer. Because of the refraction, the beam pass through the sample at an angle β, as defined in Eq. (1a).

For LDPE and LLDPE, $n = 1.51$, and thus:

$$S_N = 4.02930(S_{TN} - 0.88358S_T) \quad (2)$$

For HDPE, $n = 1.54$, and thus:

$$S_N = 4.21364(S_{TN} - 0.88835S_T) \quad (3)$$

the isotropic spectrum was calculated by:

$$S_0 = 1/3(S_M + S_T + S_N) \quad (4)$$

Measurements were carried out on a Nicolet 170SX FTIR at a resolution of 2 cm^{-1} with an accumulation of 128 scans. Polarization of the beam was done by a zinc selenide wire grid polarizer from Spectra-Tech. Typical FTIR absorption spectra of LDPE as well as fitting curves are given in Fig. 1. MD, TD and ND spectra were quite different, confirming the different orientation characteristics with respect to the three directions. The isotropic spectrum can be obtained by averaging MD, TD and ND spectra.

2.4. Crystalline morphology

Samples with 20 min of etching were examined using both FE-SEM S-4700 or Jeol JSM-6100 scanning electron microscope. The etching method used was established in a previous work [15]. The lamellar morphology for the samples without etching was observed using a low voltage microscope FE-SEM S-4700 from Hitachi. This microscopy provides high resolution of 2.5 nm at a low accelerating voltage of 1 kV and high resolution of 1.5 nm at 15 kV with magnification from 20 × to 500k × . The advantage of FE-SEM S-4700 is that the crystalline morphology can be directly observed without any chemical treatment on the samples.

2.5. Tear resistance and tensile test

A standard test for tear resistance of plastic film based on ASTM D1922 was used for MD and TD tear resistance. The tensile tests were performed according to ASTM D 882-97, a standard test method for tensile properties of thin plastic sheeting. A crosshead speed of 50 mm/min and a 0.1 kN cell with rubber clamps were used. A video extensometer with 50 mm specimen gauge length and 50 mm grip separation distance was employed.

Table 2
Conditions for formation of tubular films

Materials	Draw down ratio	Blow-up ratio	Die gap (mm)	Output (kg/h)	Thickness (μm)
LDPE	23	2	1.1	20	25
LDPE	12	2	1.1	20	50
LDPE	6	2	1.1	20	100
LLDPE-O	23	2	1.1	20	25
LLDPE-O	12	2	1.1	20	50
LLDPE-O	8	2	1.1	20	75
LLDPE-B	23	2	1.1	20	25
LLDPE-B	12	2	1.1	20	50
LLDPE-B	6	2	1.1	20	100
LLDPE-M	23	2	1.1	20	25
LLDPE-M	23	2	1.1	20	50
LLDPE-M	23	2	1.1	20	100
HDPE	12	2	1.1	20	50

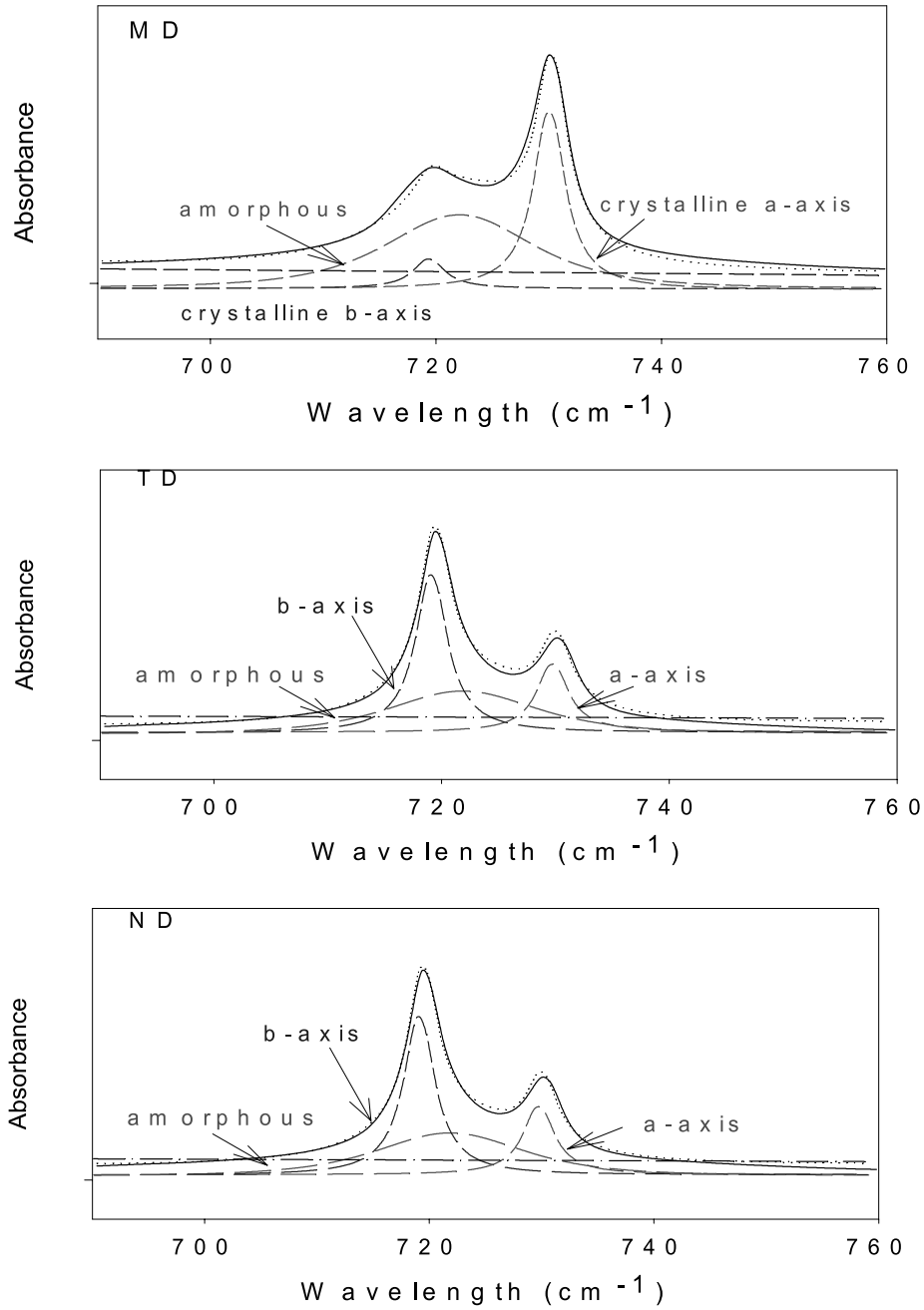

Fig. 1. FTIR spectra in machine (MD), transverse (TD) and normal (ND) directions for LDPE.

3. Results and discussions

3.1. HDPE morphologies and orientation

In the film blowing process, the orientation occurs in the melt state as a result of shear stress in the die as well as of stretching during the film blowing. Polyethylene films generally show crystalline lamellae aligned perpendicular to MD and the lamellae can be twisted or non-twisted. This particular lamellar arrangement is believed to originate from oriented high-molecular weight fraction that orient into fibrils in the film extrusion direction (MD) during the film blowing. These fibrils act as nuclei for the crystallization of the bulk. This is known as the row-nucleated structure [1]. The lamellar growth direction is the crystalline *b*-axis. Since the lamellae grow perpendicular to the primary nuclei, orientation measurement in row-nucleated blown film will show a preferential *b*-axis orientation in the direction perpendicular to machine direction (ND).

Fig. 2 shows HDPE crystalline morphology, which has a column-like morphology and lamellar orientations are perpendicular to MD. This highly ordered row-nucleated structure was formed at a medium DDR = 12, at the same condition the LDPE developed a much less row-nucleated

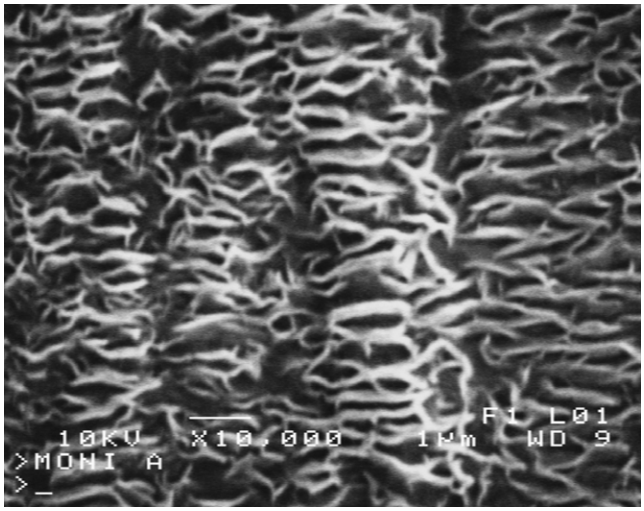

Fig. 2. Cystalline morphology of etched surface of HDPE blown film (MD ↑, TD →).

morphology while the LLDPEs formed spherulitic-structure, as showed in the following sections. It is important to note that the HDPE lamellae are non-twisted. The long connecting lines formed by meeting of lamellae grown from different nuclei are clearly observable. Separated columns with a regular period indicate the weak boundary connections between them.

Herman's orientation factors were calculated using the method described in previous studies [14,15]. Triangle plots were used to visualize the orientation characteristics of the films using the calculated Herman's orientation functions for crystalline *a*-, *b*- and *c*-axes. The three apices M, T, and N correspond to perfect orientation in MD, TD and ND, and the center corresponds to isotropic state. HDPE's MTN triangle plot is shown in Fig. 3. The orientation function values are given in Table 3. The *a*-axis is lamellar stacking direction, *b*-axis is lamellar growth direction and *c*-axis is molecular chain folded direction. The Hermans orientation function values range from $-1/2$ if the axes i ($i = a$, b, or c) and j (j = M, T or N) are perpendicular, to 0 for random orientation, to 1 when the axes i and j are parallel.

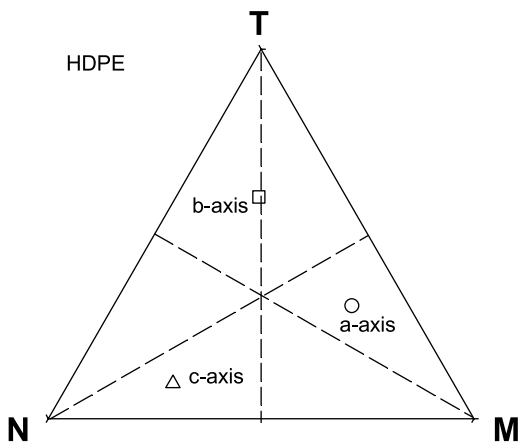

Fig. 3. MTN triangle plot for HDPE crystalline orientation (DDR = 12).

The HDPE represents a significant *a*-axis orientation in MD and *c*-axis orientation in ND. The *b*-axis orientation in the HDPE is exclusively along TD. Two distinct types of orientation can be formed in HDPE blown films depending on both blowing conditions and the type of HDPE: the first one is the one developed is under low-stress condition and related to the stress crystallization mechanism of Keller/-Machin 1 morphology, which shows the *a*-axis orientation toward MD. This is the type of orientation observed here. The second type of orientation termed high-stress crystallization or Keller/Machin 2 morphology [1,10] is analogous to cold drawn PE having substantial *c*-axis orientation along MD, meanwhile *a*-axis tends to orient to ND. This type of orientation is expected for high molecular weight HDPE blown films.

The HDPE used in this study, having relatively low molecular weight (MI = 3.4), showed row morphology and *a*-axis type orientation structure. Higher molecular weight HDPE (MI = 0.05 g/10 min [8b] and M_w = 150,000–219,000 with M_w/M_n = 10.3–15.1 [11]) could have the *c*-axis structure. According to the row-nucleated structure model, the lamellae should be twisted in Keller/Machin 1 morphology. This twisted characteristic, however, is not present in this HDPE. Actually, Keller/Machin 1 morphology neglected the possibility of *c*-axis orientation perpendicular to ND, which, in fact, was observed in some studies [4–6] as well as in this study. The *a*-axis orientation in MD and *b*-axis orientation perpendicular to MD do not necessarily result in twisting of the lamellae. The lamellae having *c*-axis randomly oriented or perpendicular to ND would be non-twisted. The twisting can be formed only if both *a*- and *c*-axes preferentially orient to MD. So it is expected the non-twisted lamellae formed in the HDPE.

3.2. LDPE morphologies and orientation

LDPE morphologies at 3 DDRs are shown in Fig. 4. It is evident that in the film plane the LDPE lamellae are oriented along transverse direction at higher DDR and relatively random at low DDR. The lamellar orientation perpendicular to machine direction (MD) is a typical morphology of row-nucleated structure [1], which becomes less distinct at lower DDR. Spherulitic crystalline morphologies were not observed even at the lowest DDR. An important feature observed at high DDR is the long and twisted nature of lamellae morphology, this is not observed for the LDPE at lower DDR. The intertwined lamellae constitute an interlocked lamellar assembly instead of well-separated rows. We call it interlocking lamellae. This structure suggests that the boundary where the lamellae meet from different row nuclei are strongly connected or overlapped by the twisted growth. The morphologies of un-etched samples were also studied (not shown here), and similarly the row-nucleated structure was observed instead of spherulitic type

Table 3
Herman's orientation functions for crystalline *a*-, *b*- and *c*-axes with respect to machine (M), transverse (T) and thickness (N) directions

Sample	DDR	*a*-axis			*b*-axis			*c*-axis		
		f_M	f_T	f_N	f_M	f_T	f_N	f_M	f_T	f_N
HDPE	12	0.3406	−0.0426	−0.2981	−0.2082	0.3997	−0.1915	−0.1324	−0.3572	0.4896
LDPE	23	0.2487	−0.1584	−0.0903	−0.4159	0.1834	0.2325	0.1672	−0.0250	−0.1422
	12	0.3236	−0.1368	−0.1868	−0.3614	0.1413	0.2200	0.0378	−0.0046	−0.0332
	6	0.1150	−0.0050	−0.1100	−0.1250	0.0400	0.0850	0.0100	−0.0500	0.0400
LLDPE-B	23	0.2994	−0.1115	−0.1879	−0.3067	0.1641	0.1426	0.0073	−0.0526	0.0453
	12	0.2618	−0.0720	−0.1898	−0.2759	0.1210	0.1549	0.0142	−0.0490	0.0348
	6	0.1256	−0.0529	−0.0736	−0.2305	−0.0070	0.2375	0.1040	0.0598	−0.1638
LLDPE-O	23	0.2398	−0.0702	−0.1696	−0.2458	0.0823	0.1636	0.0061	−0.0121	0.0060
	12	0.1359	−0.0314	−0.1045	−0.1852	−0.0120	0.1973	0.0494	0.0435	−0.0928
LLDPE-M	23	0.1460	−0.0376	−0.1084	−0.1689	−0.0008	0.1697	0.0229	0.0384	−0.0613
	12	0.1150	0.0100	−0.1250	−0.0650	0.0550	0.0100	−0.0500	−0.0650	0.1150
	6	−0.0099	−0.0354	0.0453	−0.0301	0.0103	0.0198	0.0400	0.0250	−0.0650

morphology. Both the lamellar orientation perpendicular to MD and the twisted nature are the characteristics of Keller/Machin 1 morphology, this will be further confirmed by FTIR analysis.

The triangular plot for the LDPE at three DDRs is shown in Fig. 5. The digital numbers shown in the plot are DDRs. At the highest DDR (23), the *b*-axis orientation function is strongly negative respective to MD and relatively balanced in regard of the two other directions. This means that the *b*-axis, i.e. lamellar growth direction, orients perpendicular to MD in the ND–TD plane. While *a*-axis and *c*-axis are both preferentially oriented toward MD. Among the three axes orientations, the strongest one is the *b*-axis, and the *a*- and *c*-axes tend to rotate around lamellar growth direction. The overall orientation for both *a*- and *c*-axes is toward MD. The tendency of both the *a*- and *c*- axes orientations in the same direction (MD) and *b*-axis in the direction perpendicular to MD will result in the lamellar twisting. This FTIR result is in line with morphological observation. This type of crystalline orientation is exactly what Keller row-nucleated structure model (Keller/Machin 1 morphology) predicts. As lower DDR (12, 6) were used, the *b*-axis orientation decreases correspondingly, which is in agreement with the less ordered row-nucleated morphology observations in Fig. 4. The *b*-axis are oriented perpendicular to MD and are oriented in both TD and ND for all three DDRs, which means the row-nucleated morphology are formed at all studied conditions, but with very different ordered levels. No general rule was observed for the *a*-axis orientation with varying the DDR. The *c*-axis orientation becomes isotropic at lower DDR, this corresponds to the non-twisted lamellar morphology.

3.3. LLDPE morphologies and orientation

Morphologies for both etched and un-etched samples were shown in Fig. 6. By contrast to HDPE and LDPE, the 3 LLDPE morphologies presented display spherulite-like superstructure and relatively random lamellar arrangements. Row-nucleated morphology is not achieved even though the highest possible DDR and very low frost-line were used. Such superstructure has been observed in the investigations of a Ziegler–Natta catalyzed LLDPE blown film [16] and metallocene-catalyzed LLDPE blown films [17]. The narrow molecular-weight distribution metallocene polyethylene and two other Z/N catalyzed LLDPE tend to form spherulite-like superstructure in the blown film. Little difference can be observed in the morphology of those LLDPEs films and therefore further analysis using FTIR are required to differentiate the morphologies in terms of crystalline orientation.

The triangular plots for the LLDPEs are shown in Fig. 7. At same processing conditions LLDPEs and LDPE show comparable level of the *a*-axis orientation, the LLDPEs, however, generate much weaker *b*-axis orientation in the direction perpendicular to MD. The *a*- and *b*-axes orientations indicate that LLDPEs spherulites are not in isotropic state, instead, regional orientation exists. A composite spherulitic model seems more appropriate, the orientation can be due to both the locally row-nucleated structure and *trans*-crystallization. The overall combination generates small *b*-axis orientation perpendicular to MD and *a*-axis along MD. Some results in literature on LLDPE blown films also indicated the *b*-axis orientation in the direction perpendicular to the stress, while no obvious row-nucleated morphology was visually observable in microscopic results [17–19].

The LLDPE-O and LLDPE-B show a similar trend: *a*-axis orients toward MD and tends to decrease with decreasing DDR; the *b*-axis orients perpendicular to MD with relatively balanced distribution in the TD and ND at high DDR, while decreasing DDR increases the *b*-axis orientation in ND at expense of that in TD. The negligible orientation of the *c*-axis at high DDR becomes, somehow,

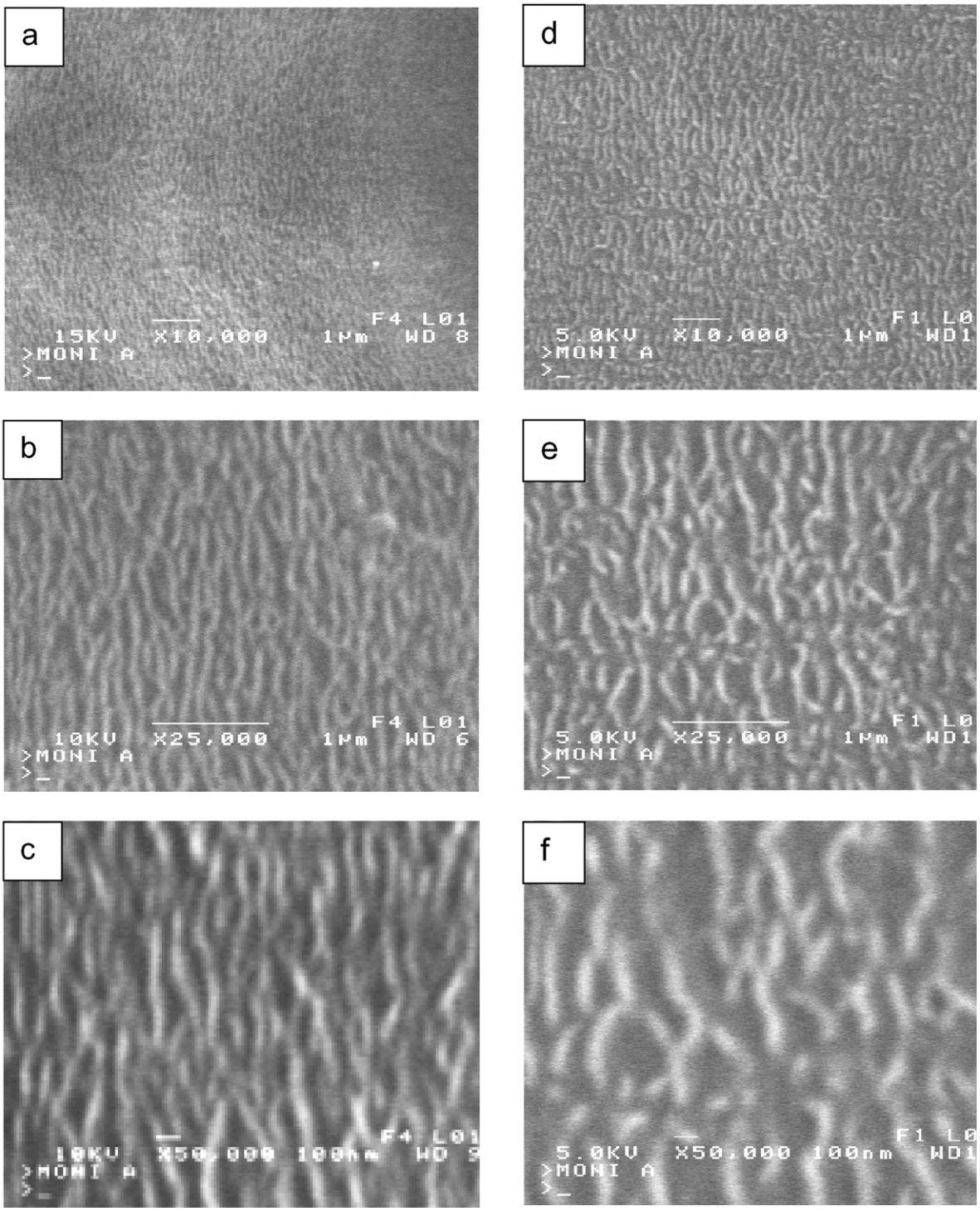

Fig. 4. Cystalline morphology of etched surface of LDPE blown films: (a, b, c) DDR = 23; (d, e, f) DDR = 12; (g, h, i) DDR = 6 (MD →, TD ↑).

biaxially oriented in the film plane as DDR decreases. The *b*-axis orientation in ND and the *a*- and *c*-axes orientation in the film plane are the characteristics of transcrystalline morphology, which becomes stronger at lower DDR. Transcrystalline morphology is formed with the preferential nucleation at surface of the film and crystal growth in the thickness direction. Nucleating sites along the surface as well as rapid cooling of polymer melt have been proved to promote this morphology. Low DDR seems to favor transcrystalline morphology. The LLDPE-M shows the lowest orientation among the 3 LLDPEs, no *b*-axis orientation along TD was observed, and the lamellae are oriented toward ND and the *a*- and *c*-axes orient in the film plane at DDR = 23, which is transcrystalline morphology.

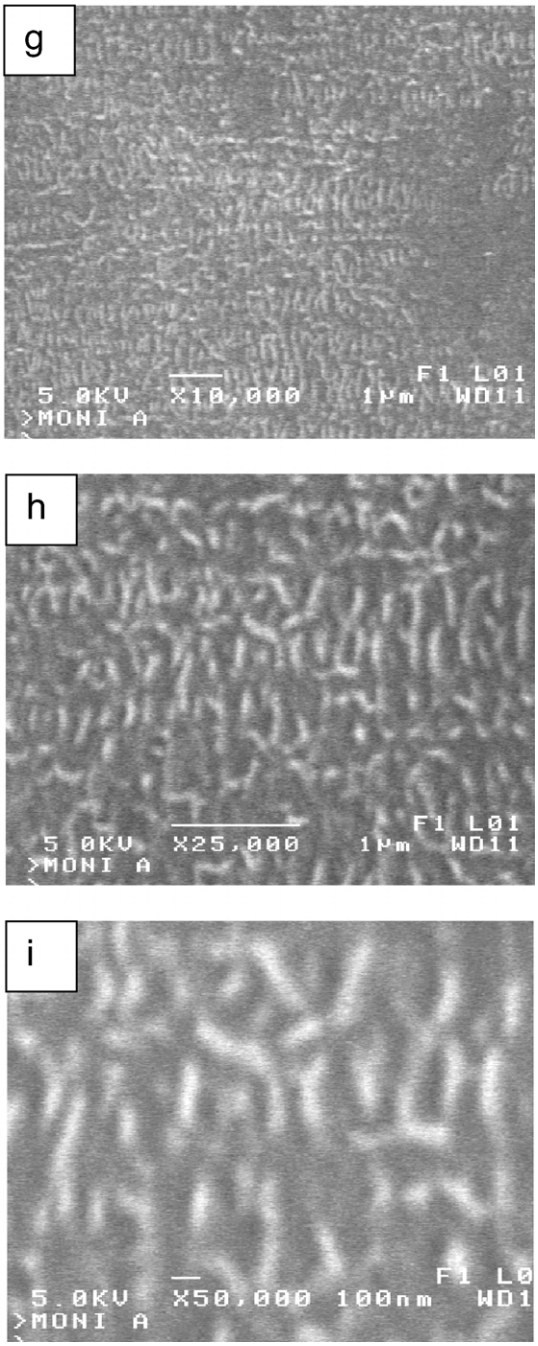

Fig. 4 (*continued*)

3.4. Effect of relaxation process on crystalline morphology and orientation

The orientation and morphological differences are thought to originate from the rheological characteristics. The logarithmic plots of complex viscosity vs. frequency at temperature of 200 °C are shown in Fig. 8. At low shear rates, HDPE has the highest viscosity and the LLDPEs, the lowest. The viscosity of LDPE is higher than, at low shear rate, those of LLDPEs, while the inverse behaviour is observed at high shear rates. The LDPE and LLDPEs showed cross-over points. Furthermore it is observed that the LLDPEs are more Newtonian at low shear rates than the LDPE and HDPE, which may be due to their narrower molecular weight distribution. The transition from Newtonian plateau to shear thinning region takes place at higher frequency for the LLDPEs than for LDPE and HDPE. From the transition frequency, the sequence of relaxation time can be estimated: HDPE > LDPE > LLDPEs.

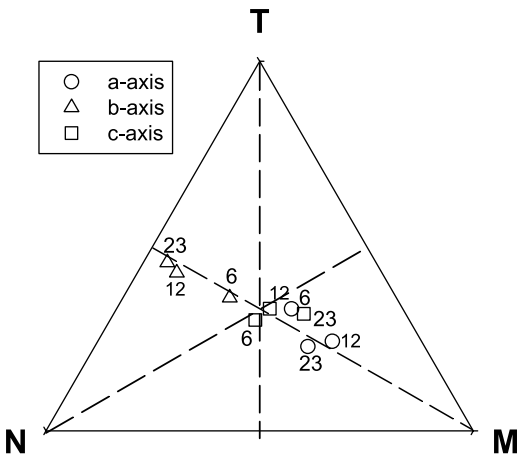

Fig. 5. MTN triangle plot for LDPE crystalline orientation. The digital numbers in the plots are DDRs.

The complex viscosity $\eta^*(\omega)$ was defined as [20]:

$$\eta^*(\omega) = G^*(\omega)/j(\omega) = \eta'(\omega) - j\eta''(\omega)$$

with

$$\eta'(\omega) = G''(\omega)/\omega$$

Table 4
Relaxation time determined by Cole–Cole plot

Resins	Temperature (°C)	Relaxation time (s)
LDPE	170	25.13
	200	10.00
	230	2.51
LLDPE-O	170	0.63
	200	0.41
	230	0.25
LLDPE-B	170	0.25
	200	0.16
	230	0.10
LLDPE-M	170	0.16
	200	0.10
	230	0.06
HDPE	170	>100
	200	>100
	230	>100

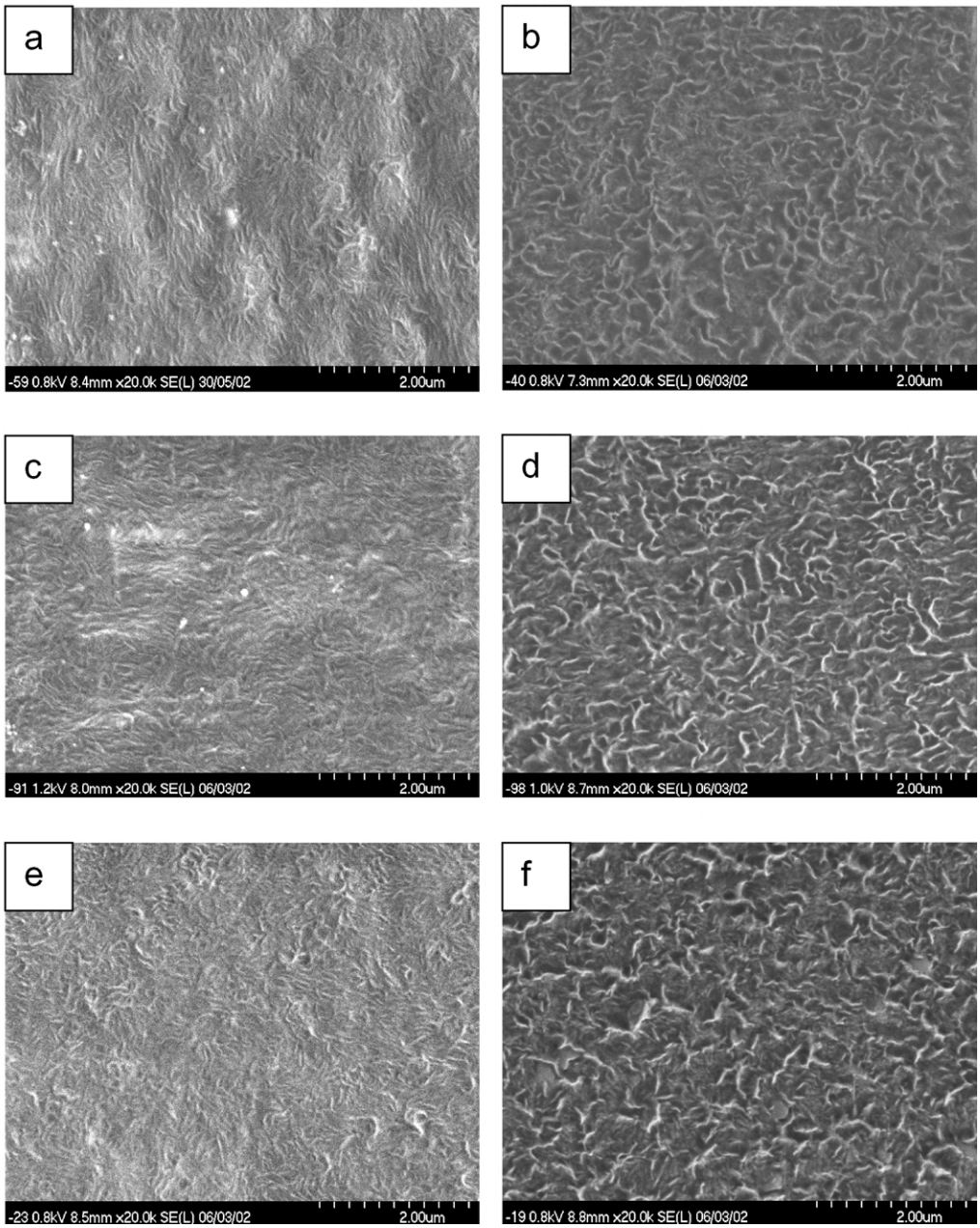

Fig. 6. Crystalline morphology of (a,b) LLDPE-O; (c,d) LLDPE-B and (e,f) LLDPE-M at DDR = 23. a, c and e are untreated surface morphologies, b, d and f are the morphologies of the etched samples (MD ↑, TD →).

and

$$\eta''(\omega) = G'(\omega)/\omega$$

The viscoelastic parameters can be derived from the log plot of $\eta'(\omega)$ vs. $\eta''(\omega)$ known as the Cole–Cole plot (Fig. 9) [20]. Cole–Cole representation of the rheological results can be visualized as a distribution of relaxation time. A characteristic relaxation time $\tau_0 = 1/\omega_c$ where is ω_c the frequency corresponding to the maximum η'' can be obtained, as described in literature [20]. The relaxation times are presented in Table 4. It is evident that LLDPEs have the lowest relaxation times, and the HDPE the highest. The relaxation times are sensitive to the temperatures, and molecular chains relax fast at higher temperature. LDPE and the LLDPEs get relatively closer at 230 °C, while the HDPE still remains with a slow relaxation.

These differences in the relaxation times may have significant role in determining the final morphology. Two steps may take place in the orientation-induced crystallization during the film extrusion process: (1) orientation-induced structure (nuclei) in the melt at the pre-crystallization stage; and (2) subsequent morphological development based on the first stage nuclei. The final morphology should be mainly dominated by the structure formed in the melt at the initial

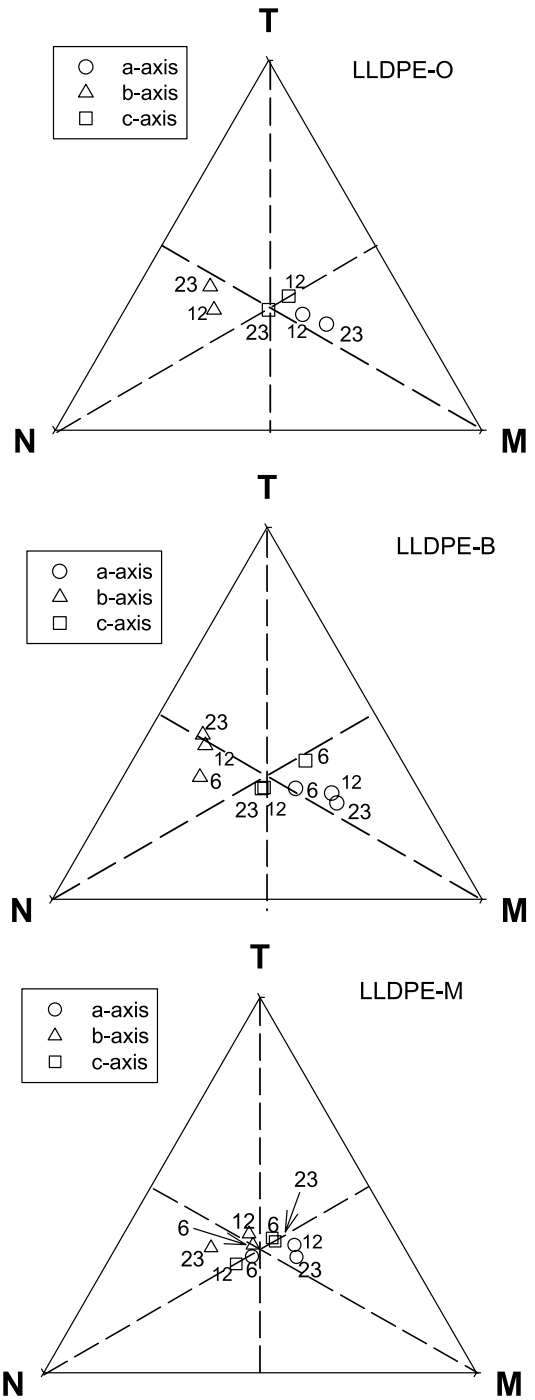

Fig. 7. MTN triangle plot for LLDPEs crystalline orientations. The digital numbers in the plots are DDRs.

stages of crystallization. The chain orientations are formed in the melt state as a result of shear stress in the die and drawing stress. Those chain orientations, however, may relax partially or completely before the onset of crystallization depending on the molecular structure and processing conditions. Only highly oriented structure from high molecular weigh fraction along MD persisting up to the frost line can serve as nuclei to promote the row-nucleated structure.

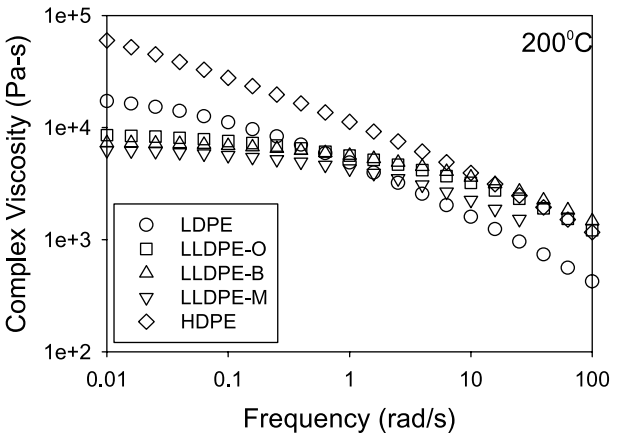

Fig. 8. Complex viscosity vs. frequency for LDPE, 3 LLDPEs and HDPE.

The row-nucleated structure contains two types of elements: a small fraction of fibrillar crystals (row nuclei) and normal type of folded chain lamellae. The presence of extended-chain fibrillar structure which serves as nuclei for lamellar oriented crystallization are prerequisite for a row-nucleated structure. Their presence determines, more than any other single factors, whether the sample will crystallize spherulitically or in a row-nucleated structure.

Since the same output, blow-up ratio and lowest frost-line height were applied to all the films, the final structure would be determined by both the stress and the relaxation time of the materials. The relaxation time is proportional to η_0 and entanglement density, and decreases with increasing temperature [21,22]. It is expected that the long chains (high molecular weight) can achieve high degree of chain alignment in the flow, since it will take a longer time for relaxation than the shorter molecular chains.

The HDPE has longer relaxation time, some chains remain highly oriented at the time of crystallization to promote row-nucleated structure. Higher crystallization temperature is another factor to get less-relaxed fabrillar nuclei for HDPE. So the row-nucleated structure was obtained in the HDPE blown film even at a medium DDR.

Table 5
Tear resistance of the polyethylene blown films

Resins	DDR	MD tear resistance (g/μm)	TD tear resistance (g/μm)
LLDPE-O	23	14.52 ± 0.58	24.57 ± 0.45
LLDPE-O	12	18.39 ± 1.65	24.51 ± 0.80
LLDPE-O	8	20.79 ± 1.54	25.15 ± 0.89
LLDPE-B	23	6.18 ± 0.64	15.86 ± 0.55
LLDPE-B	12	6.85 ± 0.80	12.45 ± 0.69
LLDPE-B	6	6.38 ± 0.15	6.46 ± 0.32
LLDPE-M	23	10.57 ± 0.65	15.40 ± 1.50
LLDPE-M	12	12.99 ± 0.37	15.41 ± 0.48
LLDPE-M	6	15.13 ± 0.54	17.99 ± 0.69
LDPE	23	13.43 ± 0.57	3.07 ± 0.13
LDPE	12	9.62 ± 0.63	4.30 ± 0.20
LDPE	6	6.79 ± 0.94	7.41 ± 0.18
HDPE	12	0.60 ± 0.13	20.73 ± 1.71

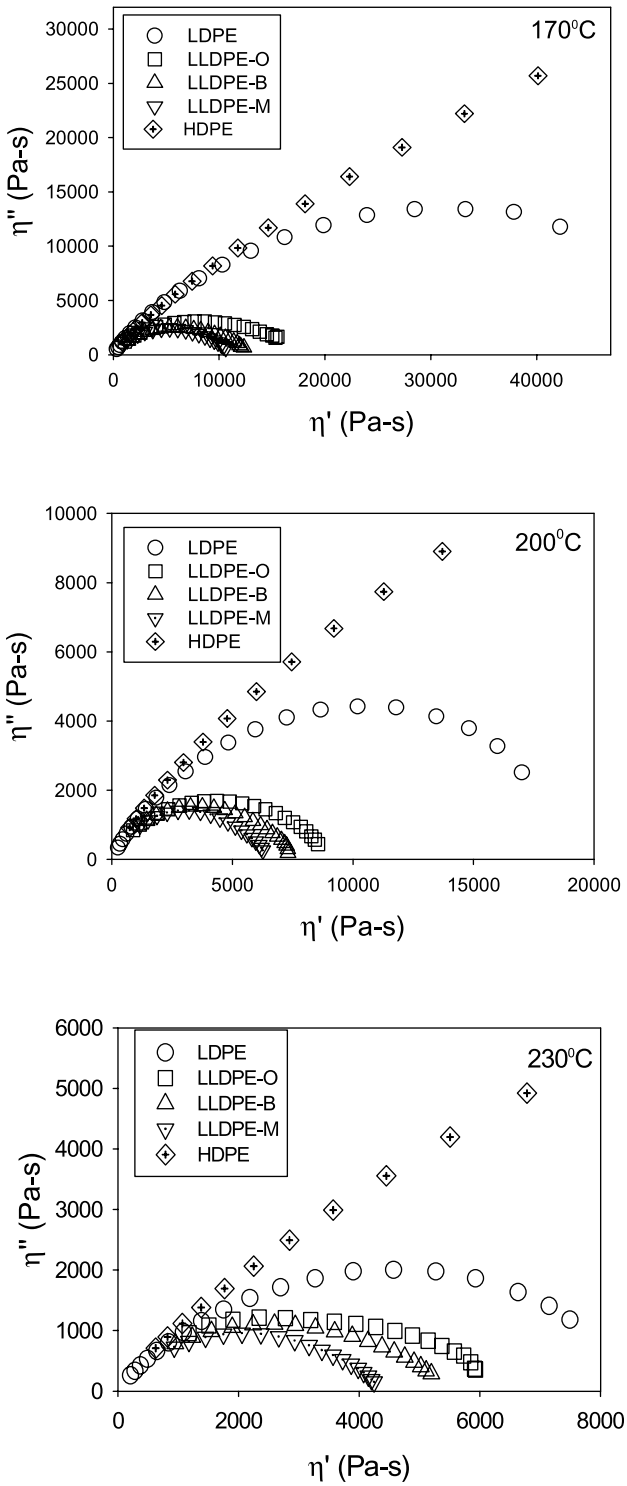

Fig. 9. Cole–Cole plot for LDPE, LLDPEs and HDPE at 200 °C.

This type of morphology is generally observable for most HDPE blown films.

LDPE generally has a higher melt entanglement and strain hardening upon melt extension due to the presence of the LCB. A recent study [23] showed the η_0 and breadth of relaxation spectrum increase with degree of LCB. This combines with longer relaxation time in LDPE leaves

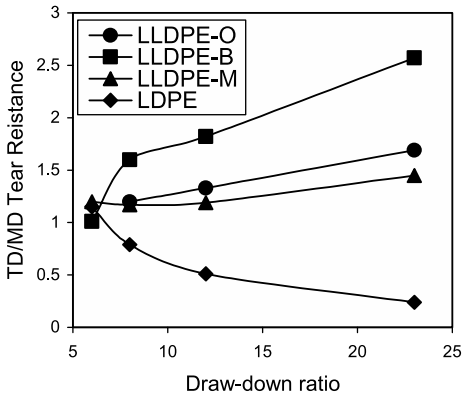

Fig. 10. Anisotropy of tear strengths.

sufficient highly oriented fibrillar nuclei to promote the row structure over the spherulites, high DDR favours formation of high level of row-nucleated morphology.

The low shorter relaxation time determine that the oriented melt of LLDPEs under stress can relax back to a low orientation or isotropic state before crystallization starts. Therefore, the LLDPEs have less chance to form highly oriented fibrillar nuclei, either the highly oriented fibrillar nuclei relaxed completely or the remaining fibril length are too short to suppress spherulite-like structure and to form row-nucleated structure. It seems difficult to obtain a row-nucleated morphology for most of the film extrusion grade LLDPEs, like the three showed in this work [24], however, a few cases showed row-nucleated morphology were the LLDPE with high molecular weight and broader distribution (MI = 0.22) [8a].

3.5. Correlation between structure and properties

Tear resistance of LLDPEs, LDPE and HDPE are reported in Table 5. As mentioned in introduction, the HDPE showed a high tear resistance in TD and an extremely low one in MD. A reverse trend is observed in the case of LDPE with tear resistance being high in the MD direction and low in TD direction. LLDPEs showed tear resistance

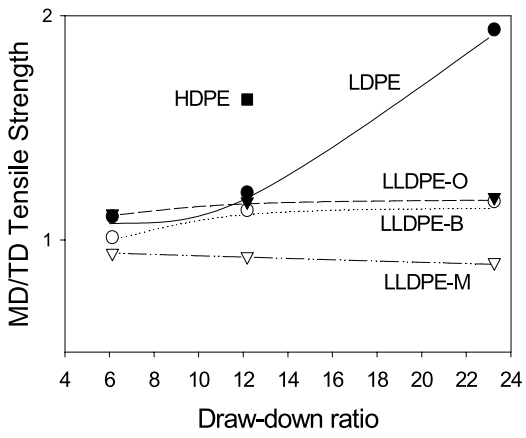

Fig. 11. Anisotropy of tensile strengths.

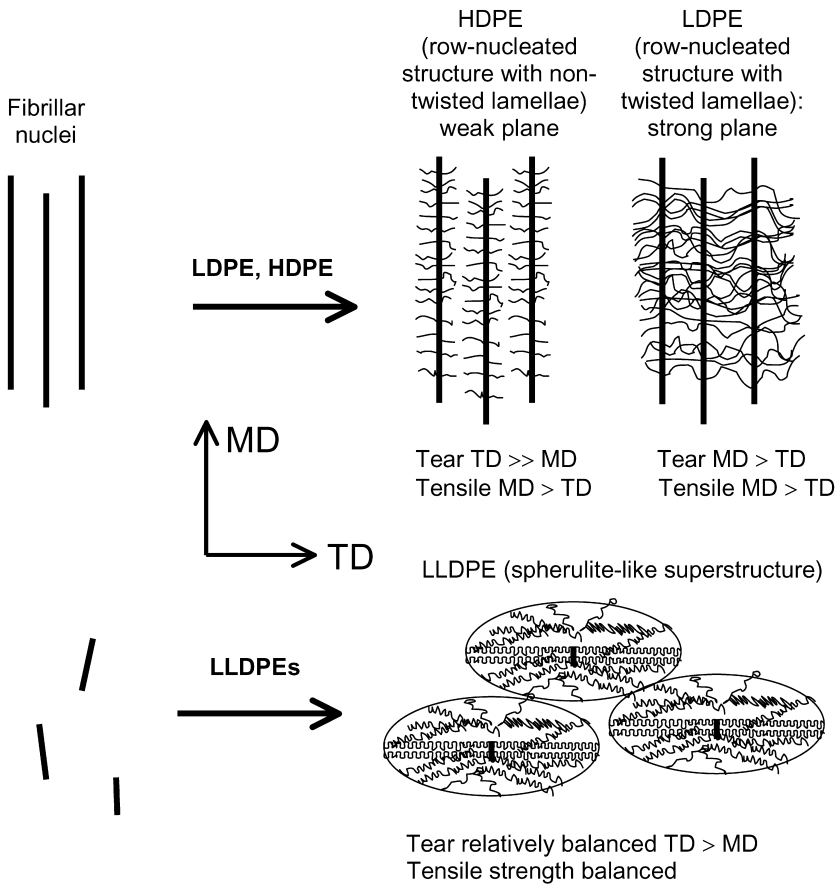

Fig. 12. Schematic of morphological developments and structure-tear resistance relationship for LDPE, LLDPE and HDPE.

larger in the TD direction than in the MD one. LLDPE-O has the best tear resistance among the 3 LLDPEs. LLDPEs, especially LLDPE-O and LLDPE-M, showed a relatively balanced tear resistance. Keeping other processing parameters constant, an increase in DDR will increase the level of orientation. The anisotropy of tear resistance can be quantified by TD/MD tear strength ratio. A plot of DDR vs. the ratio of TD to MD tear resistance was shown in Fig. 10. At low DDR, LLDPEs and LDPE have TD/MD ratio close to 1, which means low orientation resulting in a balanced tear resistance in MD and TD. As DDR increase, 3 LLDPEs show the same trend: the higher the orientation, the higher TD tends to be over MD. A reversing trend for LDPE: the higher the orientation, the higher MD over TD. The biggest tear anisotropy is seen in the HDPE.

The anisotropy can also be seen in the tensile properties, as shown in Fig. 11 for the MD/TD tensile strength of the various films. At DDR = 12 higher MD strength over the TD one is observed in the HDPE, all other films remain relatively balanced. At DDR = 23 the LDPE exhibits a strong anisotropy on tensile strength, while all LLDPEs are still well balanced in MD and TD.

We tried to link the tear resistance behaviour with tie molecular structure. Compared with crystalline orientation, much lower amorphous phase orientation was observed (not shown here): HDPE and LLDPE showed slight orientation toward MD, and LLDPEs are isotropic. The orientation results of amorphous phase were not enough to account for the big difference in tear behaviour.

The observed difference in tear resistance can be associated with the crystalline lamellar structure formed in the film process. The relationship between structure and tear anisotropy is illustrated in Fig. 12. In the LDPE film the twisted lamellae from adjacent row nuclei are strongly connected, resulting in an interlocking lamellae structure. This is responsible for the observed MD > TD tear resistance. This anisotropy decreased and even disappeared when the lamellae became less interlocked or randomly aligned at lower DDR. The row-nucleated morphologies are also present in the HDPE blown film, but separated rows result in a weak column boundary due to the non-twisted lamellae. Accordingly a very low tear resistance in MD and a higher one in TD are expected. LLDPEs showed a relatively balanced tear resistance since less oriented structure involved. The local preferential orientation of lamellae along TD allowed TD tear > MD tear for LLDPEs. The stronger tensile strength in MD over TD is attributed to the fibrillar structure, which serves as nuclei.

The anisotropy of tensile strength are indication of the presence of fibrillar structure in the HDPE and LDPE, not in the LLDPEs.

4. Conclusions

(1) The type of orientation obtained is strongly dependent on the type of polyethylene as well as the processing conditions used in the blowing process. Distinct orientation structure and morphology are found for LDPE, 3 LLDPEs and HDPE. LDPE formed a row-nucleated structure with twisted lamellae at high DDR, lowering DDR can dramatically reduce the ordered lamellar morphology. The HDPE, at a medium DDR = 12, already formed a row-nucleated structure showing non-twisted lamellar orientation in TD, *a*-axis orientation in MD and *c*-axis orientation in ND. Spherulite-like superstructures were found in the 3 LLDPEs at all processing conditions, the variations of DDR change the amounts of trans-crystalline orientation. The DDR (proportional to the stress applied in MD) as well as the resin's relaxation time play a crucial role in determining the structure formation.

(2) The interlocked twisted lamellar assembly is responsible for the enhancement of MD tear and MD > TD tear resistance behavior of the LDPE. The separated column-like morphology and weak plane in MD for HDPE lead to an extremely low MD tear and high TD tear. Preferential orientation of crystalline *b*-axis in TD generates a higher TD tear. LLDPEs were however more balanced in terms of tear properties than the LDPE and HDPE. The anisotropy of tensile properties are due to the fibrillar structure, which is present in the LDPE and HDPE but not in the LLDPEs.

(3) *a*-Axis orientation toward machine direction does not necessarily mean row-nucleated structure and twisted lamellae, it may be row-nucleated structure with twisted lamellae as predicted by Keller's model (LDPE), or spherulitic-like structure (LLDPEs), or even row-nucleated structure with non-twisted-lamellae (HDPE). It depends on the level of *b*-axis's orientation and *c*-axis's location.

Acknowledgements

The authors wish to thank Desgagnes, Dominique for FTIR measurements.

References

[1] Keller A, Machin MJ. J Macromol Sci (Phys) 1967;B1:41.
[2] Holmes DR, Miller RG, Palmer RP, Bunn CW. Nature 1953;171:1104.
[3] Lindenmeyer PH, Lustig S. J Appl Polym Sci 1965;9:227.
[4] Holmes DR, Palmer RP. J Polym Sci 1958;31:345.
[5] Aggarwal SL, Tilley GP, Sweeting OJ. J Appl Polym Sci 1959;1:91.
[6] Desper CR. J Appl Polym Sci 1969;13:169.
[7] Lu J, Sue HJ. Macromolecules 2001;34:2015.
[8] (a) Lu J, Sue HJ, Rieker TP. J Mater Sci 1996;35:5169. (b) Lu J, Sue HJ, Rieker TP. Polymer 2001;42:4635.
[9] Pazur RJ, Prud'homme RE. Macromolecules 1996;29:119.
[10] Maddams W, Preedy J. J Appl Polym Sci 1978;22:2721. see also 2739 and 2751.
[11] (a) Yu TH, Wilkes GL. Polymer 1996;37:4675. (b) Yu TH, Wilkes GL. J Mater Sci 1998;33:287. (c) Yu TH, Wilkes GL. J Rheol 1996;40(6):1079.
[12] Kwack TH, Han CD, Vickers ME. J Polym Sci 1988;35:363.
[13] Cole KC, Ben Doly H, Sanschagrin B, Nguyen KT, Ajji A. Polymer 1999;40:3505.
[14] Cole KC, Ajji A. In: Ward IM, Coates PD, Dumoulin MM, editors. Characterization of orientation in solid phase processing of polymers. Munich: Carl Hanser Verlag; 2000.
[15] Zhang XM, Verilhac JM, Ajji A. Polymer 2001;42:8179.
[16] Jordens K. SPE ANTEC 2002;1233.
[17] Johnson MB, Wilkes GL, Sukhadia AM, Rohlfing DC. J Appl Polym Sci 2000;77:2845.
[18] Hoffman JK, Miller RL, Marand H, Roitman DB. Macromolecules 1992;25:2221.
[19] Lu J, Sue HJ. J Polym Sci, Part B: Polym Phys 2002;40:507.
[20] Labaig JJ, Monge Ph, Bendarick J. Polymer 1973;14:384.
[21] Graessley WW, Segal L. Macromolecules 1969;2:49.
[22] Uy WC, Graessley WW. Macromolecules 1971;4:458.
[23] Wood-Adams PM, Dealy JM, Willem deGroot A, David Redwine O. Macromolecules 2000;33:7489.
[24] Krishnaswamy RK, Sukhadia AM. Polymer 2002;41:9205.